Solvent Extraction Research and Development, Japan, **Vol. 31, No 2, 67 – 75 (2024)**

Extraction of 5-Hydroxymethylfurfural under Hydrogen Peroxide in Liquid–Liquid Slug Flow of Water / Methylisobutylketone Biphasic System and Effect of Hemin

Toshinori SHIMANOUCHI[1,*], Sota SANAGI[1], Satoko FUJIOKA[2], Koichi TERASAKA[2] and Yukitaka KIMURA[1,*]

[1]*Graduate School of Environmental and Life Science, Okayama University, 3-1-1 Tsushimanaka, Okayama, Okayama 700-8530, Japan;* [2]*Department of Applied Chemistry, Keio University, 3-14-1, Hiyoshi, Kohoku-ku, Yokohama, 223-8522 Japan*

** Corresponding authors: tshima@cc.okayama-u.ac.jp (T. Shimanouchi); yktkkimu@cc.okayama-u.ac.jp (Y. Kimura)*

(Received October 10, 2023; Accepted February 19, 2024)

Continuous extraction process of 5-hydroxymethylfurfural (HMF) in the liquid-liquid slug flow of water/methyl isobutyl ketone (MIBK) formed in the microcapillary was examined under hydroperoxide (H_2O_2) as a reactive oxygen species (ROS). Addition of H_2O_2 reduced the extracted amount of HMF into the MIBK phase. However, the addition of hemin recovered the HMF extraction. This probably resulted from the competitive binding of H_2O_2 and HMF to hemin. The binding of hemin to H_2O_2 and HMF contributed to anti-ROS activity and an accelerated mass-transfer of HMF, respectively.

1. Introduction

5-Hydroxymethylfurfural (HMF) is one of the many potential platform chemicals for a biorenewable chemicals production [1] because an oxidation of HMF yields 2,5-furandicarboxylic acid which is a promising alternative monomer for terephthalic acid used to produce polyethylene terephthalate [2]. It is also well-known that HMF is an intermediate in the dehydration reaction for fructose, glucose, and xylose [3-5]. HMF can be directly obtained by the hydrothermal conversion from cellulose [6]. Hydrothermal processing of cellulose tends to generate the reactive oxygen species (ROS) including superoxide ($O_2^{\cdot-}$), hydroxyl radical ($^{\cdot}OH$), and hydrogen peroxide (H_2O_2). This is because intermediates such as monosaccharides, obtained from cellulose, bears the reactive oxygen functional groups such as hydroxyl/phenolic, carbonyl, or carboxylic groups [7,8]. It is mentioned that active oxygen is involved in the production of hydrochars [9]. Apart from that, a use of liquid-O_2 gas slugs under a high temperature condition (up to 165 °C) made it possible to handle the oxidation reaction of HMF into 2,5-frandicarboxylic acid [10]. Such use of slug flow as a reaction field can generate the ROS. The pulsed discharge plasma into slug flow for removal of water pollution also induced the production of ROS [11]. If the accumulation of ROS occurs during the hydrothermal processing of cellulose, the value-added intermediates including HMF might be influenced by ROS. In addition, HMF has the aromatic skeleton subject to the ROS-induced oxidation and is easily rehydrated in water [1,12,13]. Therefore, both separation of HMF from the water phase and anti-ROS treatment would be required for the robust HMF production.

For the former case, the effective separation of HMF from the water phase requires the reduction in

rehydration of HMF, which has been first achieved by the batch-typed two-phase system [1]. For a continuous production of HMF from monosaccharides such as fructose and glucose, the authors have reported the use of a liquid-liquid slug flow of water / organic biphasic system formed in the microcapillary [5,14]. The slug flow is the flow of the intermittent sequence of fluid slugs followed by another fluid. The application of slug flow has been reported [15]. For examples, the slug flow generates a vortex field, so that the mass transfer of substrates and reactions can be accelerated [16]. The methods to estimate the mass transfer of dyes has been reported by Lin *et al.* [17]. The partition behavior of 17 kinds of substrates in the slug flow has been clarified to be controlled by the change of line velocity or hydrophobic difference between water and organic biphasic systems [14]. These results give an adequate two-phase system for the reactive extraction process of substrates based on the characterization of two-phase system [14]. Therefore, use of a liquid-liquid slug flow of two-phase system is a promising approach for the effective separation of HMF.

For the latter case, the reduction in ROS can be performed by the specific enzymes and metal complexes. Catalase and superoxide dismutase are the typical enzyme with anti-ROS activity [18]. However, enzymes are not available under the hydrothermal conditions because of their denaturation. In contrast, hemin with porphyrin structure [19-21] shown in Figure 1 is well-known for metal complex with anti-ROS activity. The use of hemin is unlikely to be limited by temperature conditions including hydrothermal conditions. In an earlier study, hemin could be recovered in the membrane fractions obtained from the pathological cells [22,23] and partitioned into the liposome membrane [24]. Liposome membranes can be regarded as the water / organic biphasic system [25]. It was thus expected that hemin is a promising compound to reduce the ROS at the interface of water / organic biphasic system. However, hemin in water phase favors the dimeric form, in contrast to the monomeric form in DMSO [26]. Additionally, the dimeric form is inactive for catalytic reaction [26, 27]. Therefore, control of the association behavior of hemin in the bulk water or organic phase would allow the removal of ROS during the HMF extraction process.

In this study, we aimed to impart the anti-ROS activity to the extraction process of HMF using a liquid-liquid slug flow of water / methyl isobutyl ketone (MIBK) biphasic system (Figure 1). Hydrogen peroxide (H_2O_2) was used as model ROS. It is noted that a biphasic system of water / MIBK has been reported to be a promising extraction field for HMF [14]. The extraction behavior of HMF and its coefficient of volumetric mass transfer were characterized in the presence of H_2O_2 as ROS and/or hemin. Finally, how hemin molecules acted to an HMF for its extraction process was discussed.

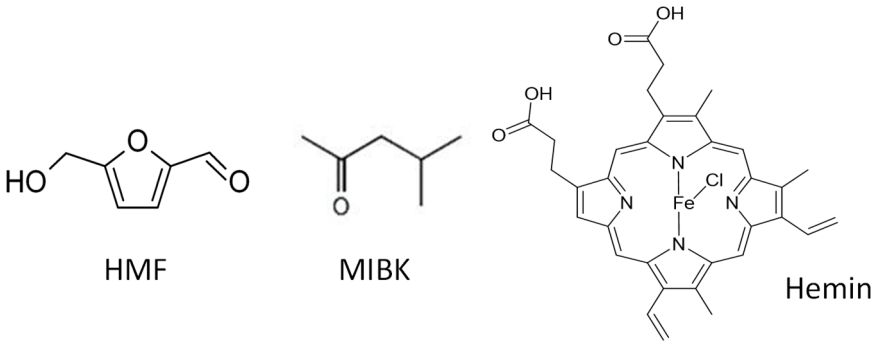

Figure 1. Chemical structures for compounds used in this study.

2. Experimental

2.1 Materials

Methylisobutylketone (4-methyl-2-pentanone; MIBK) and hemin (Mw = 651.9) were purchased from Wako Pure Chemical Industry. Ltd. (Osaka, Japan). 5-hydroxymethyl-2-furaldehyde (HMF) (99%, Mw = 126.1) was purchased from Sigma Aldrich (Tokyo, Japan). Other chemical reagents were of analytical grade. Polyetheretherketone (PEEK) and SUS tubes were obtained from GL Science, Co. Ltd. (Tokyo, Japan).

2.2 Set up of the extraction system

The flow system used in this study is shown in Figure 2 [14]. In short, hemin was first dissolved in DMSO. This solution was thereafter mixed with MIBK solvent. For the extraction experiment, the aqueous solution including 79 μM HMF with and without 1 mM H_2O_2 was thereafter injected to mix with the organic solvent MIBK including 0 – 1 mM hemin. Both aqueous and organic solution were loaded by a flow rate of 0.110 mL/min and mixed with one after another at a T-junction to form the slug flow. A flow rate ratio of organic to aqueous solution was set at 1 because the liquid-liquid extraction of HMF is promoted by the convection and vorticity in slugs at the flow rate and flow rate ratio mentioned above [14]. The mixture was kept at 25 °C in a heating bath to control the extraction process. The pressure was elevated up to 2 MPa by controlling the back-pressure valve. The tube with an inner diameter of 8.0×10^{-4} m was used in the instrument shown in Figure 2. The residence time of extraction was determined by the length of SUS316 tube immersed in heating bath. The extraction into MIBK phase was monitored for 200 sec. For a UV measurement, hemin in DMSO was injected in water with stirring. Final volume ratio of DMSO to water was set below 2 vol% to ignore the influence of DMSO.

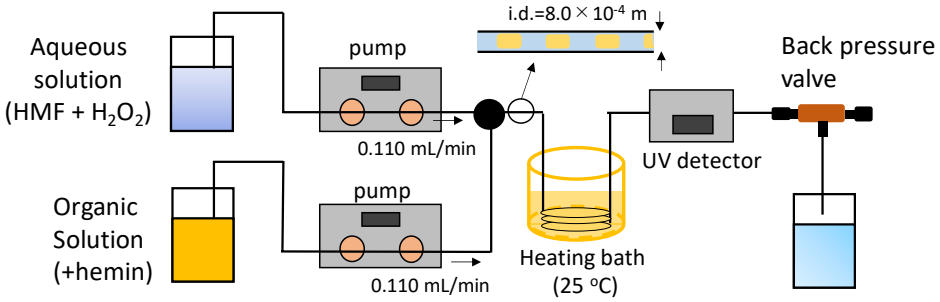

Figure 2. Experimental instruments for HMF production using the flow system.

2.3 Determination of the HMF concentration

The concentration of HMF was measured according to the previous reports [5,14]. The sample obtained from the reaction was analyzed by high performance liquid chromatography. The column used was a COSMOSIL 5C18-AR-II packed column (4.6 × 250 mm, Nacalai Tesque Co. Ltd., Japan). We added 5 μL of the sample into the column equilibrated at 38 °C wtih a flow rate of 0.80 mL/min. The mobile phase was MeOH / H_2O = 20 / 80 (wt / wt). The HMF in the sample was detected by a peak at 254 nm of wavelength, by using the photo diode array detector (SPD-M20A, Shimazu Co. Ltd.). The peaks derived from the water and the MIBK phases were eluted at 10 and 45 min.

3. Results and Discussion

3.1 Influence of H_2O_2 on the continuous extraction process of HMF

In the first series of experiments, we measured the extracted amount of HMF into MIBK phase through the continuous extraction operation by using a liquid-liquid slug flow of water/MIBK biphasic system formed in microcapillary at 25 °C (see Figure 2). An excess H_2O_2 concentration (1 mM) to achieve the HMF (79 μM)-controlled extraction process was used, assuming the generation of more H_2O_2 (model ROS) in the upstream reaction than HMF synthesis reaction. Figure 3a and b show the extracted amount of HMF into the MIBK phase and its extraction efficiency. The control system indicated 23.0 μM of HMF extracted into the MIBK phase and its extraction efficiency was 29.1%. The addition of H_2O_2 reduced the extracted amount of HMF to 15.9 μM (extraction efficiency 20.1%). Furthermore, the addition of hemin (0.1 mM) indicated the recovery of extracted amount of HMF (32.5 μM, extraction efficiency 41.2%), which was more than that for the control system. Therefore, the action of hemin to an extraction process of HMF into MIBK phase might result from not only (i) the anti-H_2O_2 activity of hemin but also (ii) accelerated mass transfer of HMF by hemin.

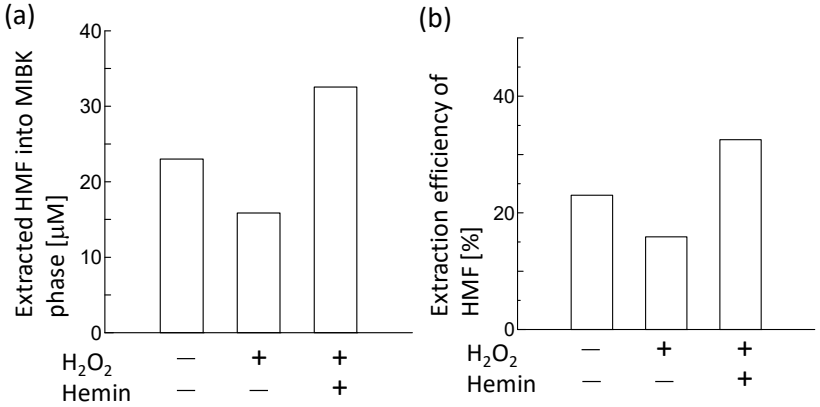

Figure 3. Continuous extraction of HMF under each condition. (a) Extracted amount of HMF into MIBK phase and (b) its extraction efficiency. Initial concentrations of HMF, hemin, and H_2O_2 were 79 μM, 0.1 mM, and 1 mM, respectively. Extraction experiment was performed at 25 °C for 100 s. Both aqueous and organic phases were mixed by 0.110 mL/min and $V_{org}/V_{aq} = 1$.

3.2 Anti-H_2O_2 activity of hemin

The factor (i), anti-H_2O_2 activity of hemin was discussed. For this, H_2O_2 concentration (1 mM) was set higher than that of hemin (0.1 mM). First, the solvation state of hemin in slug flow was examined. UV/Vis spectra for hemin in water, MIBK, and DMSO are shown in Figure 4a. It is well-known that hemin is dissolved in DMSO in a monomeric manner [26]. In this case, a Soret band was detected at 400 nm. In contrast, a Soret band with a shoulder at 400 nm was detected at 385 nm, suggesting that hemin solved in water was both monomeric and dimeric [28]. The same was true in the case on hemin dissolved in MIBK phase. Alternatively, the Q band observed at around 500 nm results from the charge-transfer band. The Q bands in water and MIBK were red-shifted from 501 to 505 nm. Next, the additive effect of H_2O_2 to hemin was examined. Figures 4b and c show the UV/Vis absorption spectra for hemin in water and MIBK phases

with and without H_2O_2. Soret band detected in the case of hemin alone suggested the heme Fe^{III} [24,27]. The addition of H_2O_2 to hemin diminished this absorption, demonstrated the chemical reaction of Fe^{III} with H_2O_2 to be converted into Fe(IV). Further addition of HMF also indicated an extremely weak absorption at 385 nm, suggesting the low solubility of hemin and formation of catalytically inactive dimers [26].

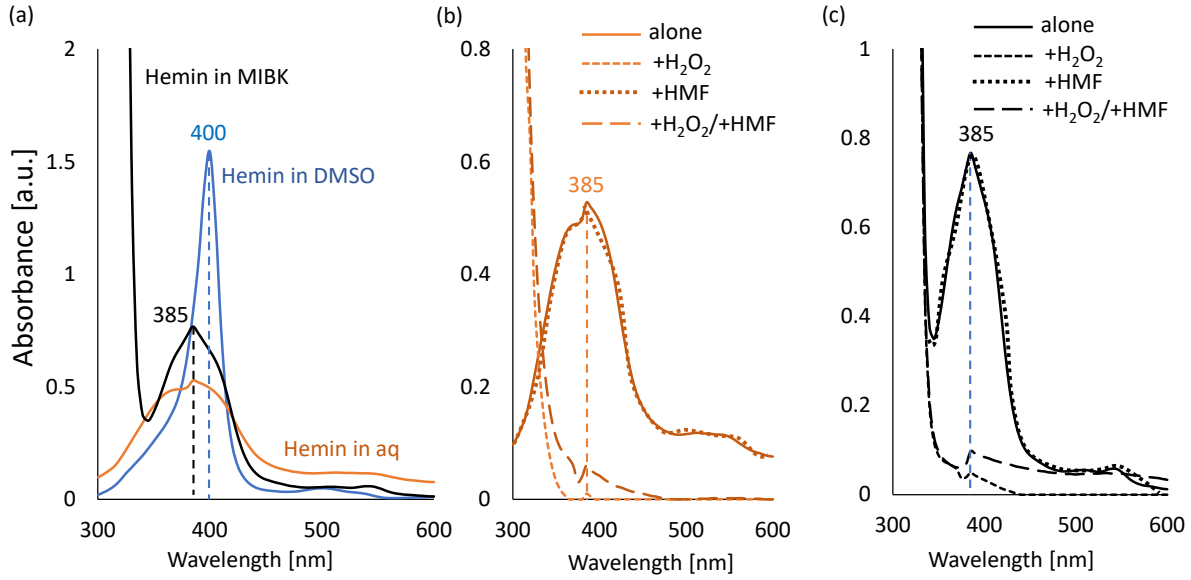

Figure 4. UV/Vis spectra for hemin. (a) Hemin in water, MIBK, and DMSO. (b) Hemin in water with H_2O_2 and HMF. (c) Hemin in MIBK with H_2O_2 and HMF.

3.3. Effect of hemin on mass transfer property of HMF

In this section, the factor (ii) was examined. The extraction process of HMF relates to its mass transfer process across the interface of the water and organic solvent. Defined the concentrations of HMF in aqueous and MIBK phases as C_A and C_R, respectively, the volumetric mass transfer coefficient for HMF (k_La) was thereby estimated by using the time-development equation (1) [30].

$$\ln\left(1-\frac{C_R}{C_A}\right)=-k_L a t \qquad (1)$$

Figure 5a shows the semi-log plots of equation (1), indicating a better correlation. The k_La values of HMF with and without 0.1 mM hemin were then 1.6×10^{-2} s^{-1} (r^2 = 0.9894) and 1.1×10^{-2} s^{-1} (r^2 = 0.9991), respectively. An increase in hemin concentration (C_H) up to 1 mM elevated k_La value (Figure 5b), suggesting that hemin molecule appeared to accelerate the mass transfer of HMF. Furthermore, the log-log plot of k_La-C_H was shown in Figure 5c, giving the linear correlation with a slope ~ 0.3 (r^2 = 0.846). This plot is called as Hill plot and the slope obtained from Hill-plot is interpreted as the cooperative binding of target with the additive. That is, the mass transfer of one HMF molecule cooperatively related with three molecules of hemin through the HMF extraction.

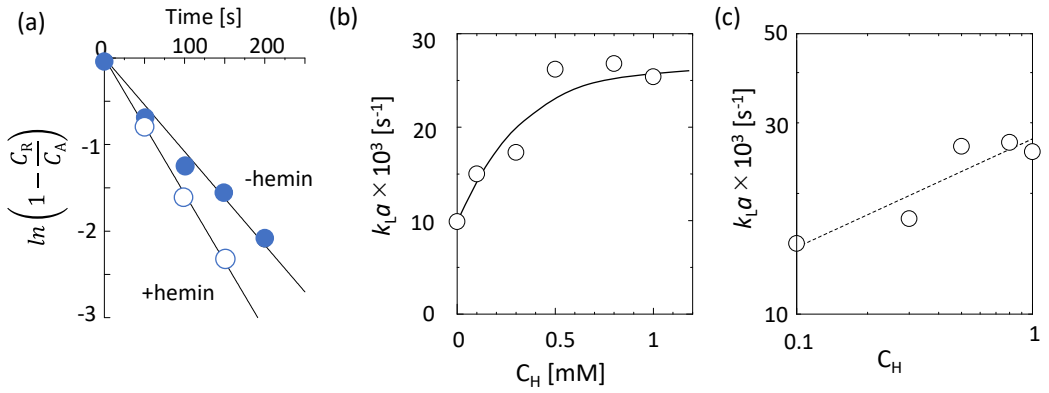

Figure 5. (a) Semi-log plots of (1-C_R/C_A) to time t. Concentration of hemin was 0.1 mM. (b) Hemin concentration dependency of volumetric mass transfer coefficient, k_La. (c) log-log plots of k_La and C_H. The slope was about 0.3 (r^2 = 0.846). C_{A0} = 79.4 μM and C_{R0} = 0 μM. Both aqueous and organic phases were mixed by 0.110 mL/min and V_{org}/V_{aq} = 1.

3.4 Analysis of extraction behavior of HMF based on a kinetic model

The analysis using k_La in the last section included the contribution of HMF rehydration and decomposition by H_2O_2. To consider these contributions to its extraction process, the facile model shown in Figure 6a was then used. This is because rehydration of HMF is slower process than the extraction process from water to MIBK phases [31]. This model that the influence of dimension of slugs dependent on the flow rate ratio of water and MIBK phase are ruled out is the simplified version of our previous model [5]. First, HMF is decomposed via both a rehydration with the rate constant k_{Rhd} and H_2O_2-induced decomposition with the rate constant k_{H2O2}. It was then assumed that the dehydration of HMF was independent of the decomposition by H_2O_2. Therefore, the overall decomposition rate was regarded as $k_2 = k_{Rhd} + k_{H2O2}$. Both A and R are defined in the eq. (1). B represents by-product obtained from HMF. And then, the reaction can be considered as the competing reaction: A ⇄ R; A→ B. Accordingly, the time variation of C_A, C_R, and C_B can be written as follows.

$$\frac{dC_A}{dt} = -k_1\left(C_A - \frac{C_R}{K_{ex}}\right) + k_2 C_A \tag{2}$$

$$\frac{dC_R}{dt} = k_1\left(C_A - \frac{C_R}{K_{ex}}\right) \tag{3}$$

$$\frac{dC_B}{dt} = k_2 C_A \tag{4}$$

$$V_{aq}C_{A0} = V_{aq}C_A + V_{org}C_R + V_{aq}C_B \tag{5}$$

where k_1, k_2 and K_{ex} represent the mass transfer coefficient of HMF from water into MIBK phases, overall decomposition rate of HMF in water phase, and partition coefficient of HMF between water and MIBK phases. From the previous study, K_{ex} = 0.91 (25 °C) [14]. V_{aq} and V_{org} are the flow rate of water and MIBK

phases, respectively.

The C_R can be then regarded as the extracted amount of HMF into MIBK phase. Then, the C_R value was monitored up to 200 s of residence time in the absence and presence of H_2O_2 and/or hemin (Figure 6b). The H_2O_2 reduced the C_R in contrast to the control system. However, the addition of hemin elevated the C_R compared with those for both control system and the condition with H_2O_2. Thereby, the time-course of C_R was fitted with equations (2) – (5) to roughly estimate the rate constant k_1 and k_2. The k_1 value in the presence of H_2O_2 ($k_1 = 1.5 \times 10^{-2}$ s^{-1}) was reduced in the case of control system ($k_1 = 3.8 \times 10^{-2}$ s^{-1}). Inversely, the addition of hemin surpassed the k_1 value ($k_1 = 7.7 \times 10^{-2}$ s^{-1}) as compared with the control system. In contrast, k_2 (= $k_{Rhd} = 7.1 \times 10^{-3}$ s^{-1}) without H_2O_2 was an order of magnitude smaller than k_1, which was in agreement with the previous report [31]. The addition of H_2O_2 elevated the k_2 (= $k_{Rhd} + k_{H2O2}$) value from 7.1×10^{-3} s^{-1} to 1.0×10^{-2} s^{-1}, probably due to the increase in k_{H2O2}. Further addition of hemin reduced k_2 value (8.0×10^{-3} s^{-1}). This was probably because of the decrease in k_{H2O2} by hemin. Thus, the increase of k_1 and reduction of k_2 by hemin suggested an accelerated effect of mass transfer of HMF from water to MIBK phase and anti-H_2O_2 effect, respectively. Therefore, the kinetic analysis demonstrated that hemin contributed to both factors (i) and (ii).

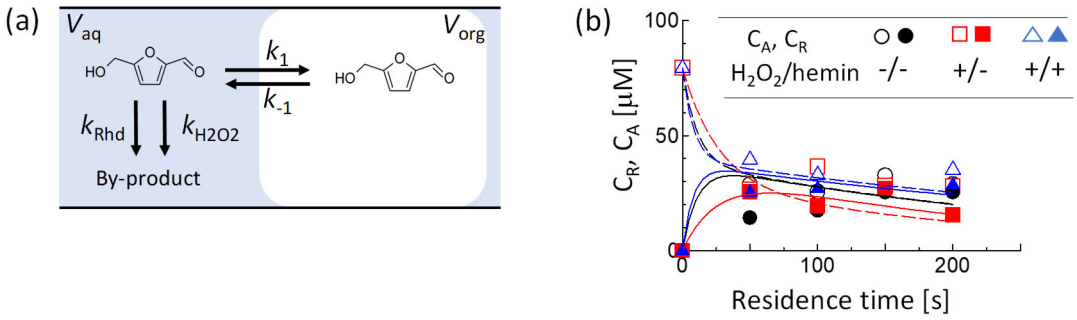

Figure 6. (a) Schematic illustration on mass transfer of HMF between water and MIBK phase. (b) Time-course of HMF extracted into MIBK phase with and without H_2O_2 and/or Hemin. Both aqueous and organic phases were mixed by 0.110 mL/min and $V_{org}/V_{aq} = 1$. $C_H = 0.1$ mM, $C_{A0} = 79$ μM, $C_{R0} = C_{B0} = 0$ μM.

3.5 Possible mechanism of hemin on HMF extraction under H_2O_2 conditions

From the experimental results regarding the factors (i) and (ii), there was a possibility that hemin molecule competitively interacted with HMF and H_2O_2. For examples, the possibility to form the π-π stacking between hemin and HMF is discussed from the UV spectra (Figure 4). The UV spectra for the specific absorbance derived from the aromatic group (380 – 390 nm) should shift to longer wavelength region, along the previous report [32]. No definite alteration for UV spectra for hemin with or without HMF was, however, observed (Figures 4b and c). This strongly suggested no formation of π-π stacking between hemin and HMF. Therefore, it was considered that hemin enhanced the mass transfer of HMF in a manner other than π-π stacking. Recently, it was clarified that hemin immobilized on graphene exerted the catalytic activity to cleavage the peroxide bond (-O-O-) because hemin could be well dispersed by π-π stacking and graphene as π donor supplied the electron to Fe^{III} by cation-π interaction [26]. Accordingly, HMF might act as π donor to supply the electron to Fe^{III} by cation-π interaction, without π-π stacking between hemin and HMF (Figure 7a). Thus, it was considered that H_2O_2 competed with HMF for binding to hemin.

Alternatively, the rehydration of HMF is discussed. A rehydration of HMF yields a variety of biproducts such as levulinic acid. Through rehydration, water molecules attack the furfural ring, hydroxy oxygen and carbonyl oxygen [33]. Hemin accelerated the mass transfer of HMF (Figure 5) and indicated an increase of k_1 (Figure 6b). It was therefore considered that Fe^{III} of hemin bound not only to oxygen of furfural ring but also to oxygens of hydroxy and carbonyl groups (Figure 7b). This was in agreement with the result of Hill-plot, *i.e.* 3:1 of hemin : HMF (Figure 5c). Furthermore, the dimeric form of hemin is stable in a solvent with high relative permittivity (like water), because the dimerization of hemin could reduce its hydrophobicity [28,34] or π-π stacking of the porphyrin rings [34]. Under the coexistence of HMF and hemin, hemin might easily form a complex structure with HMF near the interface (Figure 7b), and then decrease its hydrophobicity, which promotes mass transfer into MIBK phase.

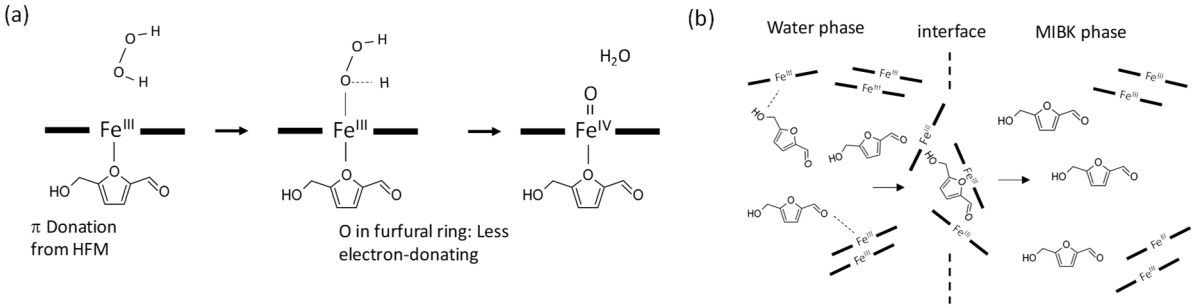

Figure 7. Possible mechanism of (a) competitive binding of hemin to H_2O_2 and HMF. The binding of π donation via O of furfural ring was drawn. (b) Hemin-induced extraction of HMF.

4. Conclusion

The extraction process of HMF in the liquid-liquid slug flow was, in this study, examined with and without H_2O_2 and hemin. In the presence of H_2O_2, the extracted amount of HMF into MIBK phase was reduced. However, the addition of hemin recovered the extracted amount of HMF. A UV spectra and Hill-plot using the volumetric mass transfer coefficient suggested competitive binding of hemin to HMF and H_2O_2. It was considered that hemin would interact with HMF in a manner other than π-π stacking. From the results, it was implied that hemin played two roles: (i) anti-H_2O_2 activity associated with HMF and (ii) improved extraction of HMF based on its accelerated mass transfer.

Acknowledgement

This study was partly supported by a Grant-in-Aid for Scientific Research (No. 23K11490) of the Ministry of Education, Science, Sports and Culture of Japan.

References

1) Y. Román-Leshkov, J. N. Chheda, J. A. Dumesic, *Science,* **312,** 1933-1937 (2006).
2) S. E. Davis, L. R. Houk, E. C. Tamargo, A. K. Datye, R. J. Davis, *Catal. Today*, **160**, 55-60 (2011).
3) F. S. Asghari, H. Yoshida, *Ind. Eng. Chem. Res.*, **46**, 7703-7710 (2007).
4) R. Weingarten, J. Cho, W. C. Conner, Jr., G.W. Huber, *Green Chem.*, **12**, 1423-1429 (2010).
5) T. Shimanouchi, Y. Kataoka, T. Tanifuji, Y. Kimura, *AIChE J.*, **62**, 2135-2143 (2016).

6) W. Yang, T. Shimanouchi, S. Wu, Y. Kimura, *Energy Fuels*, **28**, 6974-6980 (2014).
7) M. Sevilla, A. B. Fuertes, *Chem.-Eur. J.*, **15**, 4195-4203 (2009).
8) M. Sevilla, A. B. Fuertes, *Carbon*, **47**, 2281-2289 (2009).
9) S. E. Elaigwu, G. M. Greenway, *Int. J. Ind. Chem*., **7**, 449-456 (2016).
10) A. Hommes, B. Disselhorst, H. M. M. Janssens, R. J. A. Stevelink, H. J. Heeres, J. Yue, *Chem. Eng. J*., **413**, 127552 (16 pages) (2021).
11) Wahyudiono, S. Machmudah, H. Kanda, Y. Zhao, M. Goto, *Eng. J.*, **25**, 1-17 (2021).
12) M. Möller, F. Harnisch, U. Schröder, *Biomass Bioenergy*, **39**, 389-398 (2012).
13) D. Klingler, H. Vogel, *J. Supercrit. Fluids*, **55**, 259-270 (2010).
14) T. Shimanouchi, S. Fujiioka, T. Tanifuji, K. Yamamoto, K. Terasaka, Y. Kimura, *Solvent Extr. Res. Dev., Jpn.*, **28**, 21-35 (2021).
15) M. B. Plutschack, B. Pieber, K. Gilmore, P. H. Seeberger, *Chem. Rev*., **117**, 11796-11893 (2017).
16) R. Telmesani, J. A. H. White, A. B. Beeler, *ChemPhotoChem*, **2**, 865-869 (2018).
17) Y. Liu, C. Yao, L. Yang, M. Yang, G. Chen, *MethodsX*, **8**, 101346 (13 pages) (2021).
18) J. Xu, X. Duan, J. Yang, J. R. Beeching, P. Zhang, *Plant Physiol.*, **161**, 1517-1528 (2013).
19) H. Nagami, H. Umakoshi, T. Shimanouchi, *Biochem. Eng. J*., **21**, 221-227 (2004).
20) L. Lei, Q. Tu, L. Jiao, S. Xiang, L. Wang, X. Ran, B. Xiao, G. Feng, J. Feng, C. Zhang, *Chem. Eng. J.*, **432**, 134356 (12 pages) (2022).
21) B. Jiang, Y. Yao, R. Xie, D. Dai, W. Lu, W. Chen, L. Zhang, *Appl. Catal., B*, **183**, 291-297 (2016).
22) N. Shaklai, Y. Shviro, E. Rabizadeh, I. Kirschner-Zilber, *Biochim. Biophys. Acta*, *Biomembr.*, **821**, 355-366 (1985).
23) I. Kirschner-Zibler, E. Rabizadeh, N. Shaklai, *Biochim. Biophys. Acta*, *Biomembr.*, **690**, 20-30 (1982).
24) J. B. Cannon, F. S. Kuo, R. F. Pasternack, N. M. Wong, U. Muller-Eberhard, *Biochemistry*, **23**, 3715-3721 (1984).
25) R. Kuboi, H. Umakoshi, *Solvent Extr. Res. Dev., Jpn.*, **13**, 9-21 (2006).
26) T. Xue, S. Jiang, Y. Qu, Q. Su, R. Cheng, S. Dubin, C.- Y. Chiu, R. Karner, Y. Huamg, X. Duan, *Angew. Chem., Int. Ed.*, **51**, 3822-3825 (2012).
27) J. Silver, B. Lukas, *Inorg. Chim. Acta*, **78**, 219-224 (1983).
28) V. Srinivas, C. M. Rao, *Biochem. Int.*, **21**, 849-855 (1990).
29) M. J. Deka, D. Chowdhury, *J. Phys. Chem. C*, **120**, 4121-4129 (2016).
30) N. D. M. Raimondi, L. Prat, C. Gourdon, J. Tasselli, *Chem. Eng. Sci*., **105**, 169-178 (2014).
31) T. D. Swift, C. Bagia, V. Choudhary, G. Peklaris, V. Nikolakis, D. G. Vlachos, *ACS Catal*., **4**, 259-267 (2014).
32) A. Fischbacher, C. von Sonntag, T. C. Schmidt, *Chemosphere*, **182**, 738-744 (2017).
33) C. Antonetti, D. Licursi, S. Fulignati, G. Valentini, A. M. R. Galletti, *Catalysts*, **6**, 196 (29 pages) (2016).
34) A. Nath, J. A. Dharmadhikari, A. K. Dharmadhikari, D. Mathur, S. Mazumdar, *Phys. Chem. Chem. Phys*., **19**, 26862-26869 (2017).